Macromolecules **2008**, *41*, 2959−2962

Entanglement Relaxation Time in Polyethylene: Simulation versus Experimental Data

Javier Ramos,*[†,‡] Juan F. Vega,[†] Doros N. Theodorou,[‡] and Javier Martinez-Salazar[†]

Departamento de Física Macromolecular, Instituto de Estructura de la Materia, CSIC, Serrano 113 bis, 28006 Madrid, Spain, and Department of Materials Science and Engineering, School of Chemical Engineering, National Technical University of Athens, 9 Heroon Polytechniou Street, Zografou Campus, 15780 Athens, Greece

Received November 5, 2007; Revised Manuscript Received January 31, 2008

ABSTRACT: A combined computer simulation and experimental study describing the viscoelastic properties of linear polyethylene is presented. For the simulation, a set of C_{1000} polyethylene models were equilibrated using advanced Monte Carlo moves. Then, MD trajectories were calculated. From these simulations the entanglement molecular weight, M_e, and the entanglement relaxation time, τ_e, were directly obtained. By introducing the experimental value for the plateau modulus and the simulated values for M_e and τ_e into the reptation model, one finds that the derived curves of the relaxation shear modulus nicely coincide with the experimental ones.

I. Introduction

A detailed understanding of the physical properties of polymer melts is fundamental, since their behavior is directly related to the molecular architecture. A direct route connecting melt physical properties and molecular architecture is given by the linear viscoelastic response. The whole viscoelastic fingerprint can be conveniently represented by a combination of Rouse-like models for the segmental motion at short times and the molecular theory of viscoelasticity of Doi and Edwards, based on the original reptation concept of de Gennes, at longer times.[1,2]

Currently, atomistic or coarse-grained molecular dynamics simulations can provide a good description of the Rouse regions of unentangled models and the transition to the plateau zone of entangled polymers.[3,4] However, they cannot cover the broad time domain of relaxation of high molecular weight entangled melts. In this respect, the combination of connectivity-altering Monte Carlo moves (equilibration stage) and molecular dynamics simulations (production stage) has been proved to be successful for obtaining, at the atomistic scale, the polymer features of well-entangled polymer models, i.e., the chain dimensions as a function of the chemical structure, $\langle R^2\rangle/M$, the molecular weight between entanglement points, M_e, and the entanglement relaxation time, τ_e.[5,7] In a recent paper was reported, for the first time, a Monte Carlo study of the macromolecular conformational features of linear and short chain branched polyethylene (PE) using an united-atom force field and on-purpose-designed connectivity-altering MC moves.[7] The number of skeletal carbons was held fixed at 1000, while the number of branches was systematically varied from 0 to 115. These systems are presently considered as high-quality models for the new generation of polyolefins.[7] By mapping the atomistic Monte Carlo trajectories on the packing model,[8] we derived for linear PE a value of M_e of about 710 kg/mol employing the TraPPe force field[9] and 880 kg/mol by using a more sophisticated force field.[10]

In this paper we calculate the characteristic entanglement relaxation time, τ_e, from molecular dynamics trajectories, which were previously equilibrated using Monte Carlo simulations, for a well-entangled linear PE melt. Additionally, we use the results of M_e and τ_e obtained from computer simulations, in the prediction of the linear viscoelastic response by assuming the reptation motion of polymer chains in the terminal zone, and compare the calculated relaxation modulus with experimental results for a set of materials. This mesoscopic model requires only a few molecular features, including the molecular weight distribution, the plateau modulus, G_N^0, the molecular weight between entanglements, M_e, and the relaxation time of an entanglement strand, τ_e. This relaxation time is commonly defined in terms of basic polymer features, such as the monomeric friction coefficient, ζ_0, the monodisperse ratio of chain end-to-end distance to molecular weight for an ideal equilibrium random coil, $\langle R^2\rangle/M$, the average molecular weight between topological constraints, M_e, and the molecular weight of the monomeric unit, m_0:[1]

$$\tau_e = \frac{\zeta_0 \dfrac{\langle R^2\rangle}{M} {M_e}^2}{3\pi^2 k_B T m_0} \tag{1}$$

with k_B being the Boltzmann constant and T the absolute temperature. It is worthwhile to mention that M_e and ζ_0 cannot be measured directly, and they have to be derived through the relationships established by mesoscopic tube models.[11–15]

II. Computer Simulations

A system of $n = 20$ linear chains, each comprised of $N = 1000$ segments, was used. Segments along the polymer chain are simulated by a united atom model with methyl ($-CH_3$) and methylene ($-CH_2-$) groups represented as individual interaction sites. Detailed parameters employed in this work can be found in the Supporting Information. The initial configuration of the molecular dynamics is previously equilibrated using Monte Carlo simulations. The molecular dynamics simulations are carried out under constant pressure and temperature (NPT ensemble), which was implemented via the Nosé-Hoover Langevin piston method.[16] The equations of motion are integrated with the velocity Verlet algorithm. To speed up the MD simulation, a multiple time step algorithm is used, namely the reversible reference system propagator algorithm (rRESPA).[17,18] This algorithm decouples slow and fast degrees of freedom using different Liouville operators for each of them, allowing the use of more than one time step for the time integration of the different degrees of freedom. Here, we used

---

* To whom all correspondence should be addressed. E-mail: j.ramos@iem.cfmac.csic.es.

[†] Instituto de Estructura de la Materia, CSIC.

[‡] National Technical University of Athens.

10.1021/ma702445e CCC: $40.75

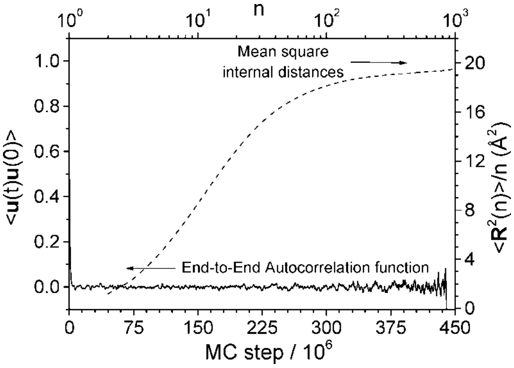

Figure 1. End-to-end autocorrelation vector $\langle \mathbf{u}(t)\mathbf{u}(0)\rangle$ (solid line, bottom and left axis) and mean-square internal distances between segments $\langle R^2(n)\rangle/n$ (dash line, top and right axis) from Monte Carlo simulations of the 20-chain C_{1000} system.

a $\delta t = 1$ fs for the bending and torsional potential and $\Delta t = 5$ fs for nonbonded interactions. The overall simulation time was 190 ns.

The decay of the end-to-end autocorrelation vector (EE-ACF) and the mean-square internal distances between segments (MSID) along the chain were followed during Monte Carlo simulations to ensure the equilibration of the melt at all length scales (see Figure 1). The EE-ACF rapidly drops to zero, indicating equilibration at the end-to-end length scale. Moreover, the MSID curve increases monotonically toward a plateau value. This behavior indicates that the chains are equilibrated at all segmental length levels. The value of the plateau is related to the stiffness of the chain. The Monte Carlo chain dimensions are mapped on the packing model equations. A similar approach has been used to explain the value of viscoelastic properties of a set of short chain branched polyolefins. A more complete description of the techniques can be found elsewhere.[7] As a summary, it could be said that this model links the size of polymer coils to the point at which the molecules entangle and, therefore, to their rheological behavior in the melt. The packing length value is defined as the occupied volume (i.e., volume per polymer molecule) divided by the mean-square end-to-end distance (squared chain size, proportional to the 2/3 power of the pervaded volume) of a chain:[8]

$$p = \frac{V_{\mathrm{occ}}}{\langle R^2\rangle} = \frac{M}{\langle R^2\rangle \rho N_{\mathrm{A}}} \tag{2}$$

or equivalently

$$l_{\mathrm{p}} = \frac{V_{\mathrm{occ}}}{\langle R_{\mathrm{g}}^{\,2}\rangle} = \frac{M/\rho N_{\mathrm{A}}}{\langle R_{\mathrm{g}}^{\,2}\rangle} \tag{3}$$

where M is the molar mass of the polymer, ρ is the melt density, and N_{A} is Avogadro's number.

Furthermore, some molecular features, such as M_{e}, are related to the packing model. Thus, it has been established that M_{e} is proportional to $\rho l_{\mathrm{p}}^{\,3}$ where the proportionally constant is independent of the temperature and polymer architecture:

$$M_{\mathrm{e}} = 1.98 N_{\mathrm{A}} \rho l_{\mathrm{p}}^{\,3} \tag{4}$$

Taking into account these relations, we have mapped the equilibrated density and radius of gyration values obtained by MC simulations onto the equations of the packing length model in order to obtain the entanglement molecular weight. The calculated values are collected in Table 1. The value of M_{e} is very close to the value calculated from primitive path reduction of atomistic Monte Carlo simulations (0.84 kg/mol)[19] and to the more recent M_0 value (0.80 kg/mol), defined as the length of a segment between links (aka entanglements) in the slip-link model.[20]

Figure 2 shows the mean-square displacement of the innermost backbone segments through the molecular dynamics trajectory, which reads

$$g_1(t) = \frac{1}{40} \sum_{i=N/2-20}^{i=N/2+19} [\mathbf{r}(i,t) - \mathbf{r}(i,0)]^2 \tag{5}$$

To get rid of effects associated with the chain ends, all curves are obtained only over the 40 innermost backbone segments for each chain.[5] The curve shows two characteristic regions. The corresponding exponents quantifying the scaling of $g_1(t)$ with t are 0.47 and 0.35, respectively. These values are close to those predicted by the reptation theory (0.5 and 0.25, respectively).[1] The arrow in Figure 2 shows the crossover between the two regimes defining the characteristic entanglement time τ_{e}, which is 1.59 ns at 450 K. This time is independent of the polymer molecular weight and stands for the onset of the tube constraint; for $t < \tau_{\mathrm{e}}$ the segment between entanglements behaves as a Rouse chain segment in free space, while for $t > \tau_{\mathrm{e}}$ this segment feels the constraints due to the tube.

III. Comparison with Experiments

The linear viscoelastic properties of the samples listed in Table 2 have been obtained in a CVO Bohlin torsion rheometer, in the parallel plates mode in the temperature range from the melting temperature to 463 K. In Table 3 we have collected the experimental plateau moduli determined by us as well as by other authors. Furthermore, in this table the calculated M_{e} and τ_{e} are also depicted. The reader is referred to previous works for experimental details.[14,15,21,22] The time–temperature superposition principle was found to apply for all the samples studied, as expected for linear homopolymers. The temperature dependence of relaxation times was shown to obey an Arrhenius-type equation in this temperature range.[14] The characteristic flow activation energy, E_{a}, for linear PE given by the dependence observed is 25 kJ/mol. The materials show the typical response in oscillatory shear of polymers with a linear molecular architecture and a relatively narrow molecular weight distribution. The PE2300 and PE3600 samples show a characteristic plateau in the high-frequency range, as it corresponds to ultrahigh molecular weight PE.[15] For these samples a value of the experimental plateau modulus, $G_N^0 \sim 2.04$ MPa is obtained, in agreement with recent results.[15,23] This value of G_N^0 gives rise to a M_{e} value of 1.14 kg/mol, assuming that $G_N^0 = K\rho RT/M_{\mathrm{e}}$ (with $K = 4/5$ and $\rho = 0.756$ g/cm^3 at $T = 463$ K).[2]

In order to describe the viscoelastic behavior of these samples, we have considered a simplified reptation model using the basic expression for the terminal relaxation time of a chain of molar mass, M_i, that accounts for contour length fluctuations (CLF) on the basis of the entanglement segment relaxation time, τ_{e}:[24–26]

$$\tau_{\mathrm{d}i} = 3\tau_{\mathrm{e}}\left(\frac{M_i}{M_{\mathrm{e}}}\right)\left[1 - \kappa\left(\frac{M_{\mathrm{e}}}{M_i}\right)^{0.5}\right]^2 \tag{6}$$

κ is a constant of the order unity. Doi calculated a value of $\kappa = 1.47$,[27,28] and Ketzmerick and Öttinger obtained similar results by means of equilibrium Brownian dynamics simulations.[29] We have used in our calculations the more recent value of $\kappa = 1.69$ obtained by Likhtman and McLeish.[30] The expression for $\tau_{\mathrm{d}i}$ accounts for a decrease in the relaxation time as the molecular weight diminishes, shifting its value from the theoretical predicted exponent of 3.0—which holds for very long chains—to the 3.4 value characteristic of shorter chains.[15,31] Furthermore, by means of $\tau_{\mathrm{d}i}$, which includes the CLF effect, the tube survival

Table 1. Chain Dimensions, Stiffness and Entanglement Features from Mapping of the Monte Carlo Simulation Results on the Packing Length Model[a]

force field	$\langle R^2 \rangle$ (Å^2)	$\langle R_g^2 \rangle$ (Å^2)	$\langle R^2 \rangle / \langle R_g^2 \rangle$	C_∞[d]	l_p (Å)[e]	M_e (kg/mol)[f]
Trappe-UA[b]	19805 ± 50	3299 ± 6	6.00 ± 0.03	8.34 ± 0.01	9.22 ± 0.02	0.71 ± 0.01
Karayiannis et al.[c]	19335 ± 56	3187 ± 6	6.07 ± 0.03	8.06 ± 0.01	9.54 ± 0.02	0.79 ± 0.01

[a] An ensemble of 20 linear chains each comprised 1000 carbon (united groups) units were simulated. The error was calculated as the standard error of the mean values (SEM) using SEM = SD/$\sqrt{n}$, where SD is the standard deviation and n the number of samples. [b] Parameters from ref 9. [c] Parameters from ref 10. [d] $C_\infty = 6\langle R_g^2 \rangle m_0 / M l_0^2 = 6\langle R_g^2 \rangle / N l_0^2$, where M is the molecular weight, N is the number of atoms in the chain, m_0 is the monomer molecular weight, and l_0 is the bond distance (1.54 Å in this work). [e] Packing length defined as $l_p = M/\rho N_A \langle R_g^2 \rangle$, where ρ is the melt density, whose value was calculated as 0.766 g/cm^3 by NPT-MD simulations. [f] Entanglement molecular weight estimated as $M_e = 1.98 \rho N_A l_p^3$ from ref 8.

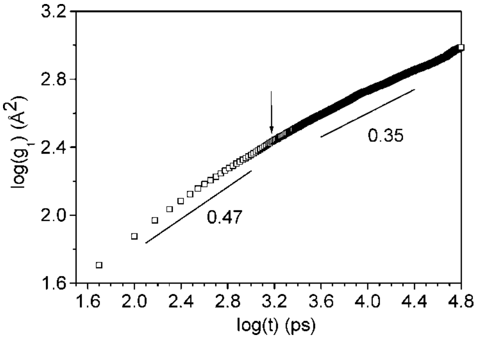

Figure 2. Mean-square displacement $g_1(t)$ of the innermost monomers as a function of the time for the PE melt here studied. Solid lines are shown to indicate the slope of each regime in the curve. The arrow indicates the onset of the effect of the tube constraints.

Table 2. Molecular Features of the Polymers Used in This Study

material	M_w (kg/mol)	M_w/M_n
HPB90[a]	90	1.1
HPB290[a]	290	1.1
PE480[a]	480	8.8
PE800[b]	800	1.8
PE1000[a]	1100	2.5
PE2300[a]	2300	2.5
PE3600[b]	3600	2.9

[a] Synthesized in our laboratory (see refs 21 and 22). [b] From ref 15.

Table 3. Characteristic Values of G_N^0, M_e, and τ_e from the Literature at 463 K[a]

reference	G_N^0 (MPa)[b]	M_e (kg/mol)	τ_e (ns)
11	2.08	1.04	7.0[c]
12	2.30	1.00	2.1[c]
13	2.60	0.86	1.45[c]
14	2.00	1.20	4.2[c]
23	2.00	1.20	
present work and ref 15	2.04	1.14	4.0
average	2.17 ± 0.23[d]		
simulation (M_e and τ_e)		0.79 ± 0.01[e]	1.3[e]

[a] The original data (at 448 K) have been shifted to 463 K by using the Arrhenius dependence of relaxation times with E_a = 25 kJ/mol. [b] $G_N^0 = 4G_e/5 = 4\rho RT/5M_e$ is the experimental "plateau" modulus. For the calculation of M_e, ρ is taken at 463 K, ρ = 0.756 g/cm^3. [c] τ_e is a parameter obtained from the fitting the experimental values to different reptation models. [d] Average of the experimental values. [e] From Monte Carlo simulation/packing model and molecular dynamics (present work).

probability of a chain i at time t, $\mu_i(t)$, can be obtained by using the expression for reptation:[1,30]

$$\mu_i(t) = \frac{8G_i}{\pi^2} \sum_{p=\mathrm{odd}} \frac{1}{p^2}\left[\exp\left(-\frac{p^2 t}{\tau_{\mathrm{d}i}}\right)\right] \tag{7}$$

where G_i is the renormalization CLF factor for the modulus:[30]

$$G_i = 1 - \kappa\left(\frac{M_e}{M_i}\right)^{0.5} \tag{8}$$

We have not included in eq 7 the early time CLF term, active at very short times (for $\tau < \tau_R$).[30] The cooperative constraint release events can be easily integrated in the model by means of the double reptation concept.[32–34] This approximation has been proved to describe reasonably well the constraint release events in the mechanical relaxation of polymer melts.[35] The effect of polydispersity can be incorporated by considering the experimental curve obtained by size exclusion chromatography, as a Gaussian function which splits up into components of molecular weight M_i and weight fraction w_i. Then, the expression for the relaxation modulus $G(t)$ for the terminal relaxation reads

$$G(t) = G_N^0\left[\sum_i w_i \mu_i(t)\right]^2 \tag{9}$$

The only unknown parameter of the model is τ_e, the characteristic relaxation time associated with the entanglement strands. The results obtained for τ_e, taken from the literature, are in reasonable agreement with those obtained in this work by direct fitting (see Table 3), but still they show some dispersion. Some authors have pointed out that τ_e is critically dependent not only on the accuracy of the model used[13] but also on the selection of polymer features such as G_N^0 and M_e, especially in the case of PE, for which a broad set of data can be found in the literature.[14,23] In addition, in the case of linear PE the characteristic relaxation time, τ_e, is not experimentally accessible by means of rheological testing, as its value falls close to the second crossover point between the G' and G'' functions at very high frequencies, in the vicinity of the Rouse regime. We have used an average value for the experimental plateau modulus of G_N^0 = 2.17 ± 0.23 MPa, obtained from all those listed in Table 3. The M_e value used has been obtained in our group by Monte Carlo, as is described in the Introduction.[7] This value is equal to 0.79 ± 0.01 kg/mol. Finally, a value of τ_e = 1.58 ± 0.12 ns has been also obtained in this work from molecular dynamics simulations at 450 K, as described in the previous section. Referred to 463 K and using the characteristic temperature dependence of linear PE, τ_e becomes equal to 1.30 ± 0.12 ns. This value is considerably lower than those calculated at the same temperature by using several fitting procedures to mesoscopic theoretical models (see Table 3). Finally, the result obtained for the relaxation modulus using the above-mentioned G_N^0, M_e, and τ_e values (see Table 3), along with the molecular features listed in Table 1, can be seen in Figure 3. The agreement between the experimental results (obtained from the measured dynamic moduli, G' and G'')[36] and the model is exceptional, taking into account the differences in the molecular weight distribution of the materials tested, including the monodisperse HPB samples. Some slight differences are expected in these cases, as the model HPB samples are not completely linear.

It should be noted at this point that the value used here for M_e is 30% lower than most typical values reported in the literature, usually in the range 1.0–1.2 kg/mol (see Table 3). The reason for the discrepancy may rely on the fact the M_e values are derived from the expression $\zeta = \rho RT/G_N^0 M_e$, where ζ takes the value of 1.25 in the Doi–Edwards theory[1] and G_N^0 is typically 2 MPa. The very recent analysis of the stress relaxation in entangled polymers of Masubuchi[20,37] and Ramírez[38] from slip-link simulations and the atomistic computer simulations

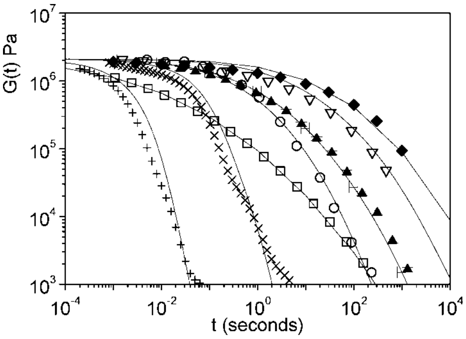

Figure 3. Relaxation shear modulus of the materials listed in Table 2 at 463 K: (+) HPB90; (×) HPB290; (□) PE480; (○) PE800; (▲) PE1100; (▽) PE2300; (◆) PE3600. The lines are calculated using the values of M_e and τ_e obtained independently from computer simulations: $M_e = 0.79$ kg/mol and $\tau_e = 1.30$ ns. The error bars in one of the materials represent uncertainty in the number of entanglements, given by the experimental molecular weight distribution uncertainty (±10%). The uncertainty in the vertical axis (modulus) is given by the experimental value of the entanglement modulus (±7%, symbol size).

from Foteinopoulou et al.[19] and Tzoumanekas and Theodorou[39] point toward higher values of the ζ parameter, between 1.4 and 2.0. The value obtained in the present work using the experimental average of G_N^0 and the value of M_e from Monte Carlo simulation gives rise to a value of 1.69, in very nice agreement with the value of $\zeta = 1.6$ recently obtained by Masubuchi et al. for linear PE.[20]

IV. Conclusions

In conclusion, the combination of advanced computer methodologies to obtain basic polymer features as the entanglement molecular weight, M_e, and relaxation time, τ_e, together with the application of a simplified topological reptation model, has allowed us strictly to explain the experimental linear viscoelastic fingerprint of a broad set of linear PE samples avoiding the use of any adjustable parameter. The computer simulations reveal for the first time the experimentally inaccessible characteristic value of τ_e for linear PE and also an inconsistency between the values of the entanglement features M_e and G_N^0 in the classical Doi–Edwards relationship. The result obtained here points toward a different prefactor value in this relationship, an idea that involves another step forward in the development of the theoretical reptation models.

Acknowledgment. J. Ramos thanks the Ministerio de Educacion y Ciencia (MEC) of Spain for financial support through a postdoctoral fellowship and the CSIC for an I3P tenure track. J. F. Vega acknowledges the MEC for a Ramón y Cajal Tenure (2006). Thanks are due to the CICYT (MAT2006-0400 project) for financial support. Authors are also grateful to Barcelona Supercomputing Center for allocation of CPU time on the MareNostrum supercomputer for the molecular dynamics simulations.

Supporting Information Available: Parameters force field used in this work. This material is available free of charge via the Internet at http://pubs.acs.org.

References and Notes

(1) Doi, M.; Edwards, S. F. *The Theory of Polymer Dynamics*; Clarendon: Oxford, 1986.
(2) de Gennes, P. G. *Scaling Concept in Polymer Physics*; Cornell University Press: Ithaca, NY, 1979.
(3) Byutner, G.; Smith, G. D. *Macromolecules* **2001**, *34*, 134–139.
(4) Byutner, G.; Smith, G. D. *Macromolecules* **2002**, *35*, 3769–3771.
(5) Harmandaris, V. A.; Mavrantzas, V. G.; Theodorou, D. N.; Kröger, M.; Ramírez, J.; Öttinger, H. C.; Vlassopoulos, D. *Macromolecules* **2003**, *36*, 1376–1387.
(6) Karayiannis, N. Ch.; Mavrantzas, V. G. *Macromolecules* **2005**, *38*, 8583–8596.
(7) Ramos, J.; Peristeras, L. D.; Theodorou, D. N. *Macromolecules* **2007**, *40*, 9640–9650.
(8) Lohse, D. J. *J. Macromol. Sci., Part C: Polym. Rev.* **2005**, *45*, 289–308.
(9) Martin, M. G.; Siepmann, J. I. *J. Phys. Chem. B* **1999**, *103*, 4508–4517.
(10) Karayiannis, N. C.; Mavrantzas, V. G.; Theodorou, D. N. *Phys. Rev. Lett.* **2002**, *88*, 105503.
(11) Pattamaprom, C.; Larson, R. G. *Rheol. Acta* **2001**, *40*, 516–532.
(12) Heuzey, M.-C.; Wood-Adams, P.; Sekki, D. *J. Appl. Polym. Sci.* **2004**, *94*, 569–586.
(13) van Meerveld, J. *Rheol. Acta* **2004**, *43*, 615–623.
(14) Vega, J. F.; Aguilar, M.; Martínez-Salazar, J. *J. Rheol.* **2003**, *47*, 1505–1521.
(15) Vega, J. F.; Rastogi, S.; Peters, G. W. M.; Meijer, H. E. H. *J. Rheol.* **2004**, *48*, 663–678.
(16) Feller, S. E.; Zhang, Y.; Pastor, R. W.; Brooks, B. R. *J. Chem. Phys.* **1995**, *103*, 4613–4621.
(17) Tuckerman, M.; Berne, B. J.; Martyna, G. J. *J. Chem. Phys.* **1992**, *97*, 1990–2001.
(18) Martyna, G. J.; Tuckerman, M. E.; Tobias, D. J.; Klein, M. L. *Mol. Phys.* **1996**, *87*, 1117–1157.
(19) Foteinopoulou, K.; Karayiannis, N. C.; Mavrantzas, V. G.; Kröger, M. *Macromolecules* **2006**, *39*, 4207–4216.
(20) Masubuchi, Y.; Ianniruberto, G.; Greco, F.; Marrucci, G. *J. Non-Newtonian Fluid Mech.,* **2008**, *149*, 87–92.
(21) Haider, N.; Expósito, M. T.; Muñoz-Escalona, A.; Ramos, J.; Vega, J. F.; Méndez, L.; Martínez-Salazar, J. *J. Appl. Polym. Sci.* **2006**, *102*, 3420–3429.
(22) Lobón-Poo, M.; Osío Barcina, J.; García Martínez, A.; Expósito, M. T.; Vega, J. F.; Martínez-Salazar, J.; Reyes, M. L. *Macromolecules* **2006**, *39*, 7479–7482.
(23) Liu, C.; He, J.; van Ruymbeke, E.; Keunings, R.; Bailly, C. *Polymer* **2006**, *47*, 4461–4479.
(24) Milner, S. T. *J. Rheol.* **1996**, *40*, 303–315.
(25) Milner, S. T.; McLeish, T. C. B. *Macromolecules* **1997**, *30*, 2159.
(26) Milner, S. T.; McLeish, T. C. B. *Phys. Rev. Lett.* **1998**, *81*, 725.
(27) Doi, M. *J. Polym. Sci., Part B: Polym. Lett. Ed.* **1981**, *19*, 265.
(28) Doi, M. *J. Polym. Sci., Part B: Polym. Lett. Ed.* **1983**, *21*, 667.
(29) Ketzmerick, R.; Ottinger, H. C. *Continuum Mech. Thermodyn.* **1989**, *1*, 113.
(30) Likhtman, A. E.; McLeish, T. C. B. *Macromolecules* **2002**, *35*, 6332.
(31) Lippits, D. R.; Rastogi, S.; Talebi, S.; Bailly, C. *Macromolecules* **2006**, *39*, 8882.
(32) des Cloizeaux, J. *Europhys. Lett.* **1988**, *5*, 437.
(33) des Cloizeaux, J. *Macromolecules* **1990**, *23*, 3992.
(34) des Cloizeaux, J. *Macromolecules* **1990**, *23*, 4678.
(35) Tsenoglou, C. *Macromolecules* **1991**, *24*, 1762.
(36) Ferry, J. D. *Viscoelastic Properties of Polymers*, 3rd ed.; John Wiley and Sons: New York, 1980.
(37) Masubuchi, Y.; Ianniruberto, G.; Greco, F.; Marrucci, G. *J. Chem. Phys.* **2003**, *119*, 6925–6930.
(38) Ramírez, J.; Sukumaran, S. K.; Likhtman, A. E. *Macromol. Symp.* **2007**, *252*, 119–129.
(39) Tzoumanekas, C.; Theodorou, D. N. *Macromolecules* **2006**, *39*, 4592–4604.

MA702445E